Hydrodynamics, H. Kim, S.H. Lee & S.J. Lee (eds) © 1998, ICHD-98 L. O. C., ISBN 89 7472 212 7

Visualization of vortical flow around breaking waves generated by a submerged cylinder using particle image velocimetry

Beom-Soo Hyun[1], Yong-Heon Shin[2] and Kyung-Shin Choi[2]

[1]Korea Maritime University, Pusan, Korea
[2]Graduate Student, Korea Maritime University, Pusan, Korea

ABSTRACT: A breaking-wave field caused by a submerged circular cylinder moving steadily under the free-surface is studied. It has been shown by Hyun and Shin (1997) that the breaking waves and the wake of cylinder interact strongly when the ratio of submergence depth and cylinder approaches approximately to 1.5. This study is designed to unveil the mechanism of interaction between breaker and cylinder using Particle Image Velocimetry (PIV) at circulating water channel. The detailed structures of the vortical flow is obtained from the velocity field measured by PIV technique. The vorticity distribution behind the breaker and cylinder well demonstrate the vortices shedded from the cylinder as well as those originated from the breaker. It has been obvious that the vortices from breaker greatly affect the whole wake field at S/D=1.

1. INTRODUCTION

The mechanism of breaking wave generated by a submerged body steadily moving under the free-surface has been undersood that the wave energy is transformed into the turbulent energy to finally dissipate into small scale turbulence. It usually occurs near the crest of gravity wave where the region of high vorticity, called "roller" or "breaker", is formed (Lee, 1997). Recent studies on wave-breaking reveal that the breaking-wave phenomena around a submerged body are governed not only by Froude number and the depth of submergence but also by Reynolds number, meaning the viscosity plays a certain role in the generation of breaking wave. Duncan (1983) confirmed the drag augmentation due to wave-breaking is attributed to a part of viscous drag by measuring the head losses around breaker. It has also been reported by Baba (1969) that the appearance of breaking wave results in the increase of ship resistance as much as 15%.

Hyun and Shin (1997) investigated the forced breaking wave by a submerged circular cylinder by measuring wave profiles, pressure distributions on body surface, head losses and turbulent intensities. It was found that the interaction between the wakes of breaker and body is the most notable feature, its pattern depending on the ratio of the depth of submergence and the diameter of cylinder. Merging of the wakes of breaker and body occurred relatively faster than could be predicted by a simple wake theory. It has been also shown that the wake of cylinder is distorted by the vortices generated by breaker so that the highly asymmetric wake distribution is produced downstream of body. Level of turbulence was also increased dramatically at and just downstream of breaker and its intensity was decreased rather rapidly, implying the rather quick dissipation of turbulent energy. Information was however restricted to time-averaged quantities so that the detailed mechanism of the interaction between the vortices shedding from body and those originated from breaker could not be clarified.

Recently, Sheridan et al. (1997) utilized the Particle Image Velocometry (PIV) technique to reconstruct the instantaneous velocity and vorticity fields generated by a cylinder, and showed the variety of interaction patterns, mainly characterized by the dramatic changes of the magnitude and direction of resultant vortical flow developed downstream of the breaker

depending on the depth of submergence as well as Froude number.

The present study aims to understand the mechanism of vortical flow in viscous flow field, and their effects on mean flow behavior to study the interaction of free surface and wake of body in more details. Presented in this paper are the results of the visualization of vortical flow structure around breaking waves and body, where mean flow as well as instantaneous flow patterns have been acquired by using PIV. It has revealed some important phenomena such as the generation and decay of vortices generated at body and free surface, and their mutual interactions as the depth of submergence varies. While PIV is definitely a powerful tool for the present purpose, further refinement of system is necessary if we want to remove all the ambiguities on the acquired images around breaker since the region of interest is quite narrow and hard to ensure enough resolution due to the reflection of light on free-surface.

2. FACILITY, MODEL AND INSTRUMENTATION

Experiment was performed in circulating water channel (CWC) with its dimensions of 5m in length, 1.8m in width and 1.2m in height. The maximum flow speed at test section is 2 m/s and the flow uniformity within 2-3% at the test section. A 7cm-diameter circular cylinder of 1m in length is made of acryl, and properly positioned at the desired depth of submergence by the 3-axis traverse system. One side of cylinder is stuck to the wall of CWC, while a thin flat plate is attached to the other side to avoid the interferences by supporting strut and other stuffs.

Flow visualization system consists of a 6W Ar-Ion Laser, fiber-optic cable and a probe with cylindrical lens for the Laser sheet generation. In order to enhance the image quality of visualization, the specially designed water-proof acryl cylinder, with a Laser sheet probe in it, was installed directly inside a test section. Vinyl chloride polymer with a specific gravity of 1.1 was used as a scattering particle, whose flow traceability was confirmed through the preliminary test in uniform flow.

Using PIV, the particle velocity of tracers, uniformly distributed in flow field, can be obtained by measuring the displacement of particle and its time interval, assuming that the trace particle is in steady linear motion during time interval between two picture frames. An 8-mm Camcorder of 1/60 sec and 640×480 pixels was used together with an image grabber to capture the instantaneous image frame at each 1/30" time step. The schematics of PIV system is shown in Fig. 1. The single exposure/double frame and cross-correlation technique was applied. That is, a captured image frame was separated into two frames, namely the odd and even fields, and the trajectory of a single particle during 1/60" was then traced by searching for the correlations between two images.

3. EXPERIMENTS

Coordinates and the schematics of breaking wave and following wavetrain are shown in Fig. 2. Here the black region denotes the breaking-wave region, and the grey the region where its influence is sustained. For the experiments, Froude number ($Fr = V/\sqrt{gD}$) was set to Fr=0.567 where V and D denote the free-stream velocity and the diameter of cylinder, respectively. The corresponding flow velocity was V=0.47m/s and the Reynolds number ($Re = VD/\nu$) was $Re=3.29 \times 10^4$. Since the aspects of wave-breaking are strongly affected by the depth of submergence of cylinder, the five different depths of submergence are considered, i.e., S/D = 2.5, 1.88, 1.43, 1.0, 0.86. Here S/D=2.5 is for non-breaking case, S/D=1.88 for condition of incipient wave breaking, and S/D = 1.0 and 0.86 for total breakdown of free-surface.

4. RESULTS AND DISCUSSIONS

Wave profiles at several S/D's are shown in Fig. 3, where the cylinder axial location and

the location of wave-breaking observed are marked also. The incipience of breaking wave is characterized by the sporadic appearance of flow instability, something like ripples, in first wave around S/D=2.15. This instability eventually become a stable breaking wave when a submerged depth is decreased to S/D=1.88. As S/D reaches less than 1.43, the breaking wave dictates all the free surface. With extremely shallow water (S/D=1), the wave-like surface profile over the body is nothing but the overflow of water over the body as like the flow over hydraulic dam. Interested reader may refer Hyun and Shin (1997) for more details.

In order to validate the accuracy of PIV system in our CWC, the preliminary measurements were made for the uniform flow as well as the lower Froude number flow. Figure 4 represents the uniform velocity field measured at the test section of CWC at V=0.47m/sec. The spatially-averaged mean velocity at test section was found to be V=0.455 m/sec, 3% lower than that by Prandtl tube. When considering the various uncertainties in CWC and the usual trend that Prandtl tube indicates 1~2% higher velocity than most of other instruments, this result serves as a good measure of the reliability of PIV system.

Another validation test is the reproduction of Karman vortex street shedding from a cylinder at several Reynolds numbers. Although Karman vortex street is not clearly shown in Fig. 5 due to the limitations of relatively small window size and high flow velocity, the diffusion of vortex street could be observed at Re = 11900, the typical phenomenon when $Re < 10^4$. All three pictures in Fig. 5 agreed qualitatively well with those presented at several bibliographies (refer van Dyke (1982) for instance). The Strouhal number at Re=32900 was obtained around St=0.17 to 0.186 depending on the way of counting the shedding frequency, presumably due to the factors such as the traceability of particle and the preciseness of image grabbing. On the other hands, the mean velocity distribution of flow field seen in Fig. 6(a) well demonstrated the wake pattern correctly, which was obtained by averaging all the instantaneous velocity fields measured for about 4 seconds.

The variation of interaction pattern between the wake of breaker and the shedding vortices from cylinder with respect to the depth of submergence can be seen in Fig. 7 to Fig. 10. For S/D=1.88 where the wave-breaking begins to be steadily visible, highly concentrated vorticity is confined very near the breaking inception point and shedded into downstream parallel to x-direction. No interaction is yet observed between the breaker and the cylinder, thus mean velocity distribution of body wake remains symmetric. Very narrow band of velocity defect is merely noticed at the downstream of breaker.

It was found in Fig. 8 for S/D=1.43 that the interaction between the wakes of body and breaker begins to play a certain role such as distortion of body wake, which can be seen in Fig. 8(a). This asymmetricity of body wake might be produced by the fact that the axis of the wake of breaker is aligned toward the depthwise direction slightly. Although its evidence could be clearly visible when observed by eye, it is not clear in Fig. 8(b) unfortunately. The region of velocity defect near free-surface behind the breaker becomes wider than at S/D=1.88.

Shallower depth of S/D = 1.0 exhibits the strong effects of breaker on body wake as in Fig. 9. Strong vorticity field generated by a breaker dramatically changes the whole flow field and develops into depthwise direction with steeper angle than that of S/D = 1.43, pushing the vortices generated at the upper side of cylinder downward and thus causing the wake of body severely asymmetric. This result is consistent with the result presented by Sheridan et al. (1997). Consequently, the velocity defect zone downstream of breaker extends widely, almost like deadzone.

Finally, for the case of S/D = 0.86 seen in Fig. 10, the wake of breaker distorts not only the vortices generated at the upper side of body, but those at the lower side. The vortices from the breaker are strong enough to create another set of vortical flow very near the free-surface. It should be noted that the vorticity as well as velocity are nearly zero in

the widely formed deadzone downstream of breaker between the vortex street produced by breaker and that of secondary vortices.

It is concluded that the present experiment well demonstrated the instantaneous flow field as well as the mean flow at several wave-breaking conditions, showing the active effect of viscosity and the strong interaction among sets of vortices. It was found that all the vortex streets developed downward with certain degrees of angle dependent upon the depth of submergence of cylinder. In order to enhance the quality of experiments, the resolution of image processing should be increased to treat the flow field more precisely, especially very near the free-surface.

5. CONCLUSIONS AND RECOMMENDATIONS

The present experimental study on the flow field around breaking waves can be summarized as follows;

(1) PIV technique has been successfully applied to research on breaking wave at CWC. The preliminary measurements made for the validation of PIV system confirm that PIV is capable of getting the mean velocity field within 3% in error and the instantaneous velocity and vorticity fields qualitatively good.

(2) The vorticity distribution behind the breaker and cylinder well demonstrated the vortices shedded from the cylinder as well as those originated from the breaker. When wave-breaking began to be steadily visible at S/D=1.88, highly concentrated vorticity was found to be confined very near the breaking inception point and shedded into downstream parallel to x-direction.

(3) Results on shallower depth clearly exhibited the strong vorticity field generated by a breaker and dramatic changes in the whole flow field. It was found that all the vortex streets developed downward with certain degrees of angle dependent upon the depth of submergence of cylinder.

(4) The resolution of image processing should be increased to treat the flow field near the free-surface more precisely.

ACKNOWLEDGMENTS

This research was supported by the Korea Science and Engineering Foundation (KOSEF) under Contract 96-0200-14-01-3.

REFERENCES

[1] Lee, S.J. (1995), "Review on the Models of Breaking Waves", *J. Research Inst. of Industrial Technology*, Chungnam Nat'l Univ., Taejon, Vol. 10, No.1, June. (in Korean)

[2] Duncan, J.H (1983), "The Breaking and Non-breaking Wave Resistance of a Two-dimensional Hydrofoil", *J. Fluid Mech.*, Vol. 126.

[3] Baba, E. (1969), "A new component of viscous resistance", J. Soc. Naval Archi. Japan, Vol.125.

[4] Hyun, B.S. and Shin, Y.H. (1997), "On Some Characteristics of Breaking Waves Generated by a Submerged Circular Cylinder", *Proc. of the 7th Int'l Symp. on Offshore & Polar Eng.* ISOPE, Honolulu, Hawaii, USA, May 25-30, 1997.

[5] Sheridan, J., J.-C. Lin and D. Rockwell (1997), "Flow Past a Cylinder Close to a Free Surface", *J. Fluid Mech.*, Vol. 330, pp. 1-30.

[6] van Dyke, M. (1982), *An Album of Fluid Motion*, The Parabolic Press, 1982.

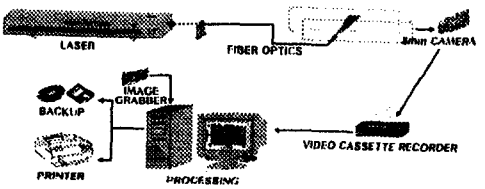

Fig. 1 PIV System

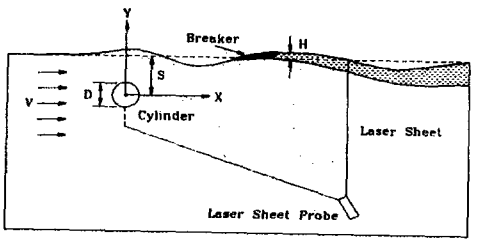

Fig. 2 Coordinates and Schematics of Experiment

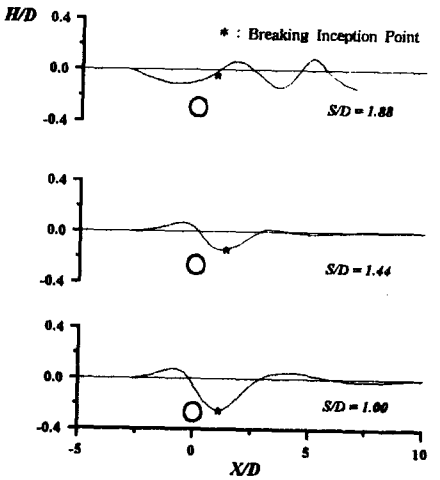

Fig. 3 Wave Profiles at Several Depths of Submergence

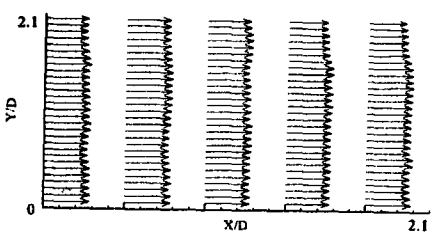

Fig. 4 Test on Uniform Flow Field

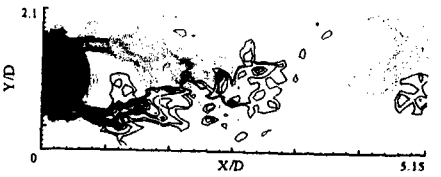

(a) Re = 11900 (Fr = 0.21)

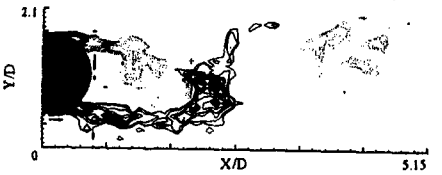

(b) Re = 18900 (Fr = 0.33)

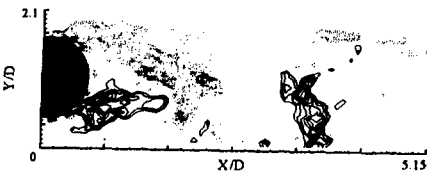

(c) Re = 32900 (Fr = 0.567)

Fig. 5 Effect of Reynolds Number on Shedding Vortices at S/D = 2.5

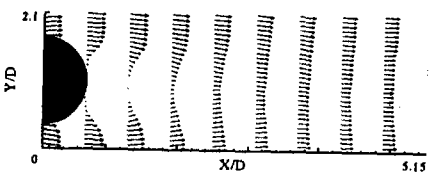

(a) Mean Velocity

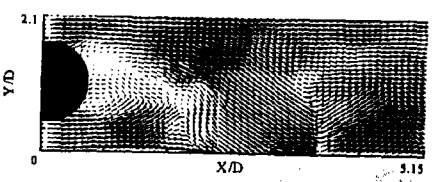

(b) Instantaneous Velocity

Fig. 6 Mean and Instantaneous Velocity Distributions at S/D = 2.5 (Re = 32900)

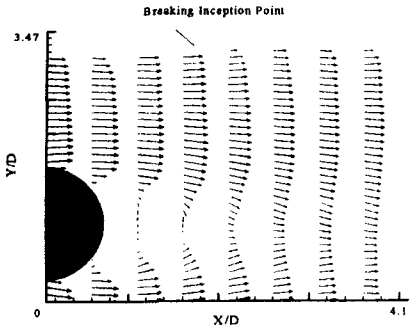

(a) Mean Velocity

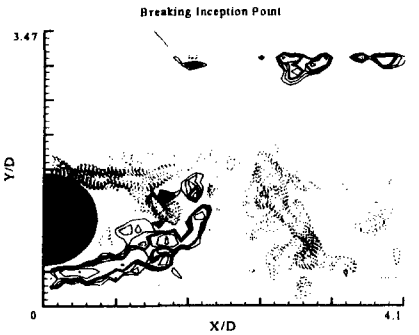

(b) Instantaneous Vorticity Field

Fig. 7 Flow Field at S/D = 1.88 (Fr=0.567)

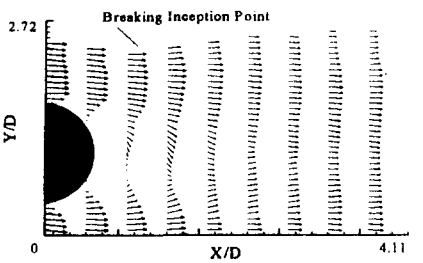

(a) Mean Velocity

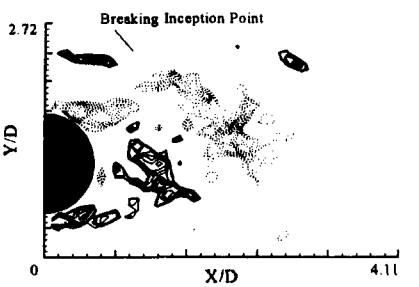

(b) Instantaneous Vorticity Field

Fig. 8 Flow Field at S/D = 1.43 (Fr=0.567)

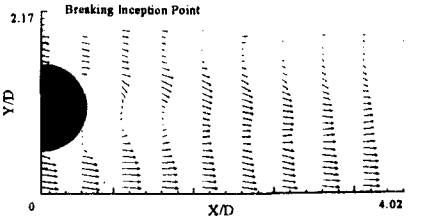

(a) Mean Velocity

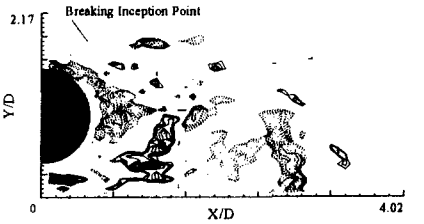

(b) Instantaneous Vorticity Field

Fig. 9 Flow Field at S/D = 1.0 (Fr=0.567)

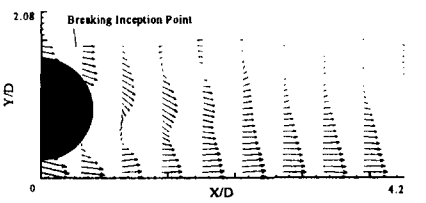

(a) Mean Velocity

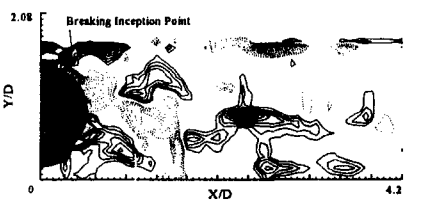

(b) Instantaneous Vorticity Field

Fig. 10 Flow Field at S/D = 0.86 (Fr=0.567)